LETTER

doi:10.1038/nature12572

Adrenaline-activated structure of β_2-adrenoceptor stabilized by an engineered nanobody

Aaron M. Ring[1,2]*, Aashish Manglik[1]*, Andrew C. Kruse[1]*, Michael D. Enos[1,2], William I. Weis[1,2], K. Christopher Garcia[1,2,3] & Brian K. Kobilka[1]

G-protein-coupled receptors (GPCRs) are integral membrane proteins that have an essential role in human physiology, yet the molecular processes through which they bind to their endogenous agonists and activate effector proteins remain poorly understood. So far, it has not been possible to capture an active-state GPCR bound to its native neurotransmitter. Crystal structures of agonist-bound GPCRs have relied on the use of either exceptionally high-affinity agonists[1,2] or receptor stabilization by mutagenesis[3–5]. Many natural agonists such as adrenaline, which activates the β_2-adrenoceptor (β_2AR), bind with relatively low affinity, and they are often chemically unstable. Using directed evolution, we engineered a high-affinity camelid antibody fragment that stabilizes the active state of the β_2AR, and used this to obtain crystal structures of the activated receptor bound to multiple ligands. Here we present structures of the active-state human β_2AR bound to three chemically distinct agonists: the ultrahigh-affinity agonist BI167107, the high-affinity catecholamine agonist hydroxybenzyl isoproterenol, and the low-affinity endogenous agonist adrenaline. The crystal structures reveal a highly conserved overall ligand recognition and activation mode despite diverse ligand chemical structures and affinities that range from 100 nM to ~80 pM. Overall, the adrenaline-bound receptor structure is similar to the others, but it has substantial rearrangements in extracellular loop three and the extracellular tip of transmembrane helix 6. These structures also reveal a water-mediated hydrogen bond between two conserved tyrosines, which appears to stabilize the active state of the β_2AR and related GPCRs.

GPCRs relay extracellular signals across a cell membrane by means of a conformational change after the binding of an extracellular agonist. GPCR activation by endogenous agonists remains poorly understood owing to the paucity of active receptor structures that have been elucidated in complex with agonists. Although a number of GPCRs have been crystallized in recent years, only the β_2AR and rhodopsin have been crystallized in fully active states[1,6], and in both cases structures are available only for complexes with a single agonist. Owing to the conformational plasticity and biochemical instability of agonist-bound receptors[7], the few agonist-bound structures of GPCRs solved thus far have relied on the use of covalent[1] or extremely high-affinity agonists[2], crystallographic chaperones to trap active states (a G protein[8] or antibody fragment[9]), or thermostabilizing mutations[3]. The last approach has only yielded structures of agonist-occupied receptor in partially active[3,4] or inactive[5] conformations.

To understand better how diverse agonists can activate a single receptor, we developed a strategy for stabilizing active-state structures of the β_2AR bound to low-affinity agonists including the natural agonist adrenaline. Here, we describe the directed evolution of Nb80, a conformationally selective single-domain camelid antibody fragment (nanobody) that was used to obtain the first active-state structure of the β_2AR[9]. Comparison with the structure of the β_2AR in complex with the G protein G_s confirmed that Nb80 stabilizes a physiologically relevant active state[8]. However, the β_2AR–Nb80 structure was of modest resolution (3.5 Å) and crystals could only be obtained with the high-affinity agonist BI167107; crystallization trials with catecholamine agonists were unsuccessful despite extensive screening. We reasoned that improving the affinity of Nb80 for agonist-bound β_2AR would decrease receptor conformational heterogeneity and enable crystallization of the receptor bound to low-affinity agonists. However, directed evolution of conformationally selective GPCR-binding proteins has never been described, probably owing to the challenges involved in biochemical manipulation of integral membrane proteins. We used yeast surface display together with a conformationally specific selection strategy to improve the binding affinity of Nb80 while maintaining its conformational selectivity. The resulting high-affinity variants retain their specificity for the active state of the receptor, which was characteristic of the original Nb80. Using the high-affinity variant Nb6B9, we determined a high-resolution (2.8 Å) active-state structure of the β_2AR bound to BI167107, and also determined the structures of the β_2AR bound to two catechol-containing agonists: hydroxybenzyl isoproterenol (HBI) and adrenaline, an endogenous low-affinity agonist of the β_2AR, at 3.1 Å and 3.2 Å resolution, respectively.

To assess the feasibility of engineering Nb80, we displayed Nb80 on the surface of the yeast strain EBY100 as an amino-terminal fusion to the yeast cell-wall protein Aga2p (Fig. 1a). Yeast displaying Nb80 were stained with purified, detergent-solubilized, biotinylated β_2AR after pre-incubation of receptor with the agonist BI167107 or the inverse agonist carazolol. Nb80-displaying yeast specifically bound to β_2AR with an overwhelming preference for agonist-occupied receptor (Fig. 1b), with a half-maximum effective concentration (EC_{50}) of 140 nM (Supplementary Fig. 1a). Next, we constructed a library of Nb80 mutants in which residues at the receptor-binding surface were randomized with conservative substitutions (Supplementary Fig. 2). The library was subjected to six rounds of selection (Fig. 1c). First, the library was positively selected with decreasing concentrations of BI167107-bound β_2AR. Before positive selection in rounds 2–5, the library was negatively selected against binding to inverse-agonist-occupied β_2AR in order to remove variants that had lost conformational specificity. For the final round of selection, we enriched variants with the slowest dissociation rates. Receptor rebinding was blocked by the addition of a large excess of soluble Nb80 after the initial receptor-binding step (Supplementary Fig. 3). This selection strategy resulted in a progressive increase in binding affinity for agonist-occupied receptor without a similar increase in binding to inverse-agonist-occupied receptor (Fig. 1d).

Nanobody 6B9 (Nb6B9) was chosen from 23 variants screened from the final round of selection (Supplementary Fig. 4) as it represented one of the highest-affinity binders tested, contained mutations that reached consensus among all sequenced clones, and was the most prevalent sequence observed. We expressed and purified Nb6B9 and Nb80, and then used surface plasmon resonance (SPR) to measure binding kinetics and affinities. Nb6B9 bound to BI167107-occupied

[1]Department of Molecular and Cellular Physiology, Stanford University, Stanford, California 94305, USA. [2]Department of Structural Biology, Stanford University, Stanford, California 94305, USA. [3]Howard Hughes Medical Institute, Stanford University School of Medicine, Stanford, California 94305, USA.
*These authors contributed equally to this work.

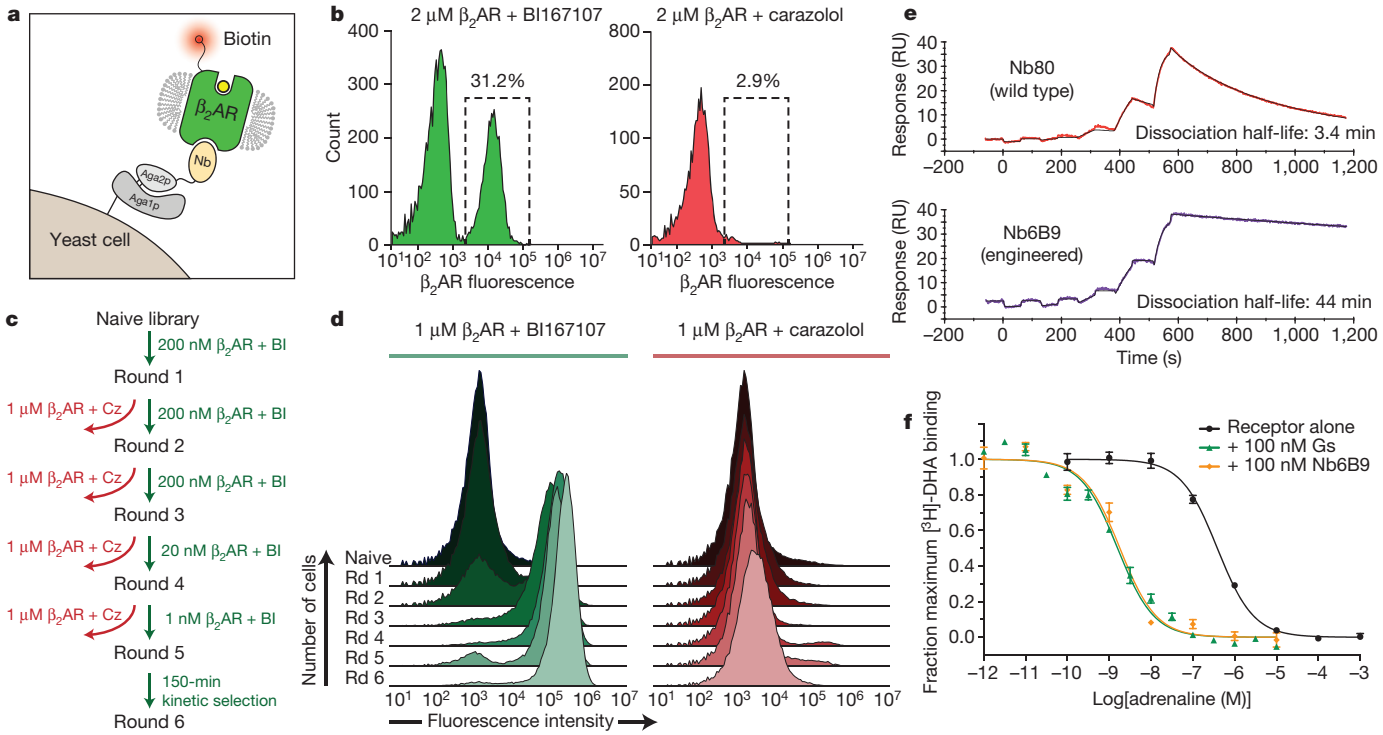

Figure 1 | Conformational selection of nanobodies and characterization of high-affinity Nb6B9. **a**, Schematic representation of yeast display of Nb80. Nb80 is fused to the N terminus of Aga2p, which attaches to the yeast cell wall through a covalent interaction with Aga1p. **b**, Staining of Nb80-expressing yeast with β_2AR bound to the agonist BI167107 (left) or the inverse agonist carazolol (right). Per cent of yeast within the boxed gate is indicated. **c**, Flowchart summary of conformational selection process. BI, BI167107; Cz, carazolol. **d**, Histogram overlays assessing β_2AR staining of the library at each round (Rd) of selection. The left panel shows staining with 1 μM BI167107-occupied receptor, and the right panel shows staining with 1 μM carazolol-occupied receptor. **e**, Representative single-cycle kinetics SPR sensorgram of wild-type Nb80 (top) and engineered Nb6B9 (bottom) binding immobilized β_2AR bound to BI167107. RU, response unit. **f**, ^{3}H-dihydroalprenolol (^{3}H-DHA) competition binding shows a comparable increase in β_2AR affinity for adrenaline in the presence of Nb6B9 as with G protein G_s. ^{3}H-DHA affinity is largely unchanged in the presence of Nb6B9 (Supplementary Table 2). Data and error bars represent the mean ± standard error of the mean from three experiments.

β_2AR with an affinity of 6.4 nM, a near tenfold improvement over Nb80 (Fig. 1e). This increase in affinity resulted from a 13-fold reduction in the dissociation rate. Competition binding experiments revealed that the β_2AR bound adrenaline with a high affinity in the presence of 100 nM Nb6B9, which is comparable to the affinity observed in the presence of the G protein G_s (Fig. 1f).

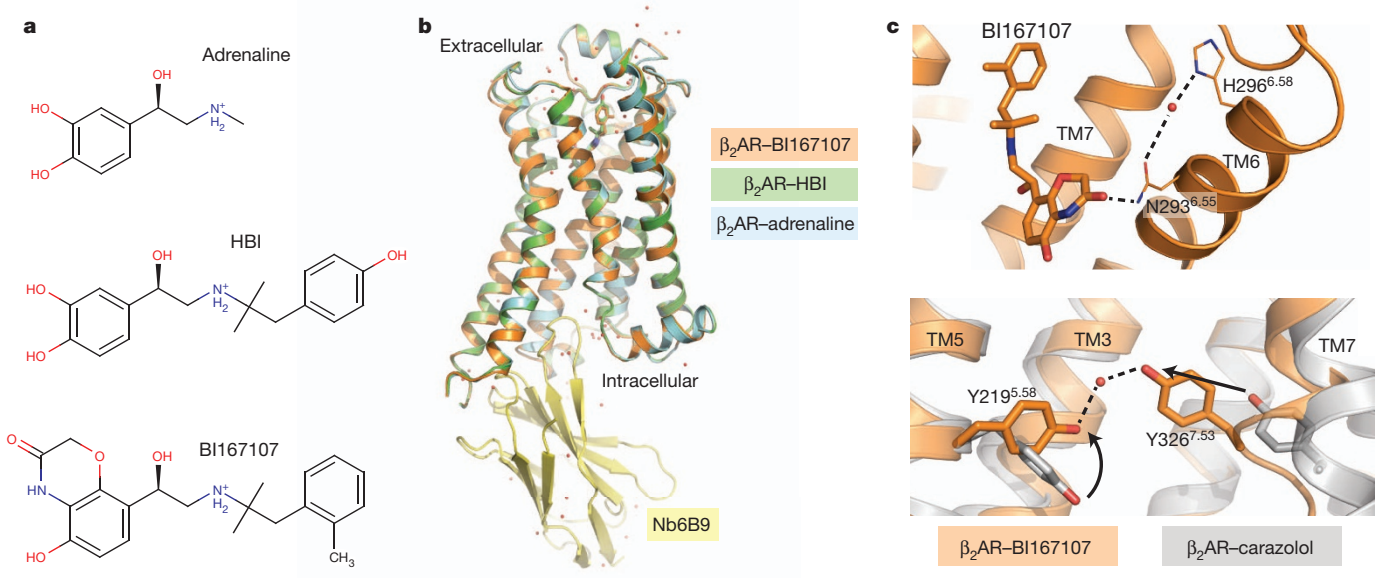

Figure 2 | Structure of the activated β_2AR in complex with three agonists. **a**, Chemical structures of the three ligands used for crystallization trials. **b**, All three active-state structures, showing remarkable similarity in overall receptor conformation. **c**, The 2.8 Å resolution structure of BI167107-bound β_2AR reveals active-state water molecules: a bridging water molecule participates in a polar network at the ligand-binding site (top) and a second water molecule mediates a hydrogen bond between two highly conserved tyrosines. Such an interaction is possible in the active state (orange) but not the inactive state (grey).

We used the lipidic mesophase method[10] to crystallize complexes of Nb6B9 with β_2AR bound to three different ligands, shown in Fig. 2a. Crystals grown with β_2AR bound to the high-affinity agonist BI167107 showed strong diffraction, and a structure was obtained to 2.8 Å resolution (Supplementary Table 1). This represents a significant improvement over the previous 3.5 Å structure of β_2AR bound to the same ligand[9]. This higher-resolution structure showed few differences from the Nb80 complex structure (Supplementary Fig. 5). Mutations in Nb6B9 appear to increase shape complementarity to active β_2AR (Supplementary Fig. 6). Many water molecules were clearly resolved for the first time, particularly in the extracellular region of the receptor (Fig. 2b, c). On the intracellular side of the receptor, a water molecule was found to mediate a hydrogen bond between Tyr $326^{7.53}$ of the NPxxY motif and the highly conserved Tyr $219^{5.58}$ on the intracellular side of transmembrane helix 5 (TM5), similar to a water seen in a recent structure of metarhodopsin II[11]. Electron density suggestive of a water molecule was also seen in HBI- and adrenaline-bound β_2AR structures, despite their slightly lower resolution. The water-mediated hydrogen bond between Tyr $219^{5.58}$ and Tyr $326^{7.53}$ is possible only in the active conformation of the receptor (Fig. 2c), and the observed water-mediated hydrogen bond may therefore contribute to active state stability in the β_2AR and other GPCRs, serving as an active-state counterpart to the 'ionic lock' that stabilizes the inactive state[12]. In support of this notion, mutation of the corresponding Tyr $223^{5.58}$ to phenylalanine in rhodopsin decreases the stability of the meta II state[13] and greatly reduces activation of transducin[14]. Moreover, mutation of Tyr $227^{5.58}$ to alanine resulted in the largest increase in thermostability for the inactive-state thermostabilized β_1AR[15].

Although BI167107 exhibits many features typical of β_2AR agonists, it lacks the catechol moiety of the endogenous agonists adrenaline and noradrenaline. Hence, it is conceivable that these agonists stabilize a different conformation of the activated receptor-binding pocket. To assess this possibility, we pursued crystallographic studies of complexes of Nb6B9 with β_2AR bound to the low-affinity endogenous agonist adrenaline and the high-affinity catecholamine agonist HBI. In each case, crystals could be grown in nearly identical conditions to those for the BI167107 complex, with clear electron density to identify the position and orientation of each ligand (Supplementary Fig. 7).

Despite the chemical diversity of these ligands, the structures of β_2AR bound to the catecholamine agonists and to BI167107 have very similar overall structures (Fig. 3a, b). A notable exception is a shift in the position of Asn $293^{6.55}$, which was previously determined to hydrogen bond with the amide carbonyl on the head group of BI167107. The smaller catechol ring of adrenaline and HBI precludes hydrogen

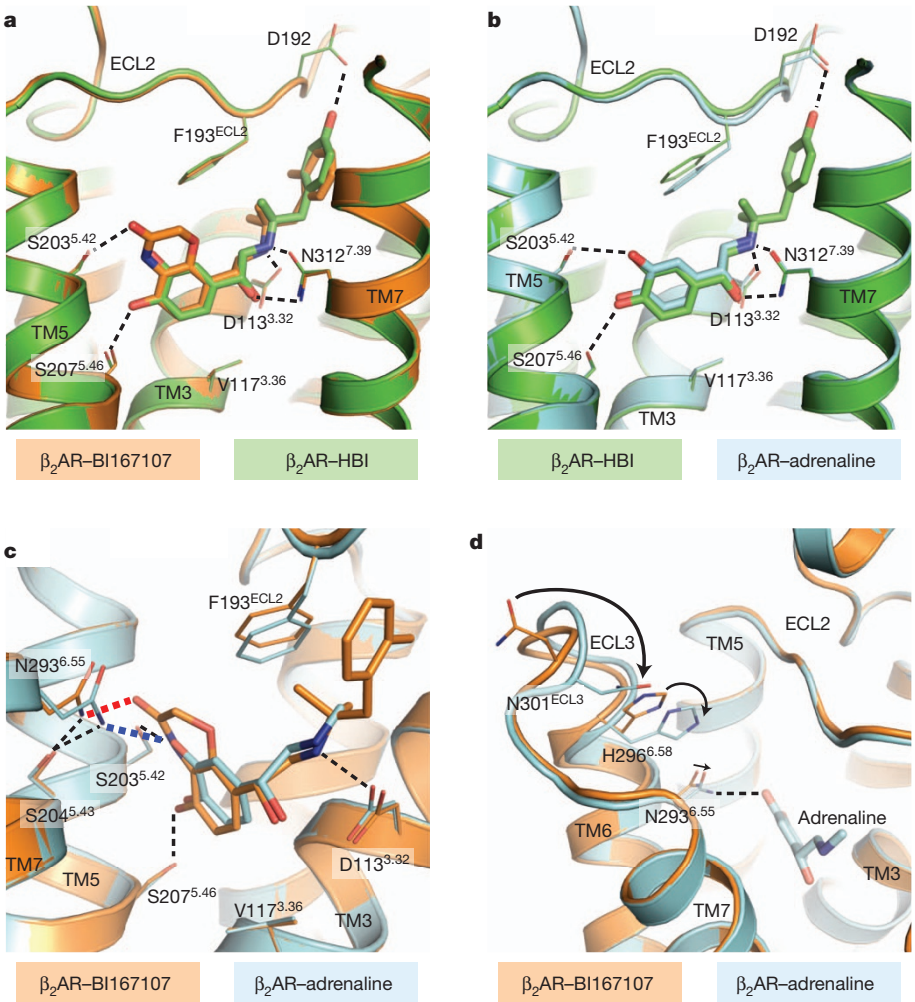

Figure 3 | Comparison of agonist-binding modes. **a**, Comparison of BI167107-bound receptor (orange) with HBI-bound receptor (green) shows a highly conserved agonist-binding mode. **b**, Similarly, adrenaline-bound (cyan) and HBI-bound (green) receptor structures are highly similar. **c**, An analogous comparison of BI167107-bound β_2AR (orange) with adrenaline-bound receptor (cyan) shows the similar polar networks for the two ligands (black dotted lines) with a notable difference in the hydrogen bonding of Asn $293^{6.55}$ to the amide proton in BI167107 (red dotted line) or the *meta* hydroxyl of adrenaline (blue dotted line). **d**, Owing to this difference, Asn $293^{6.55}$ and TM6 shift inwards in the adrenaline-bound structure, leading to a cascade of changes culminating in a rearrangement of ECL3.

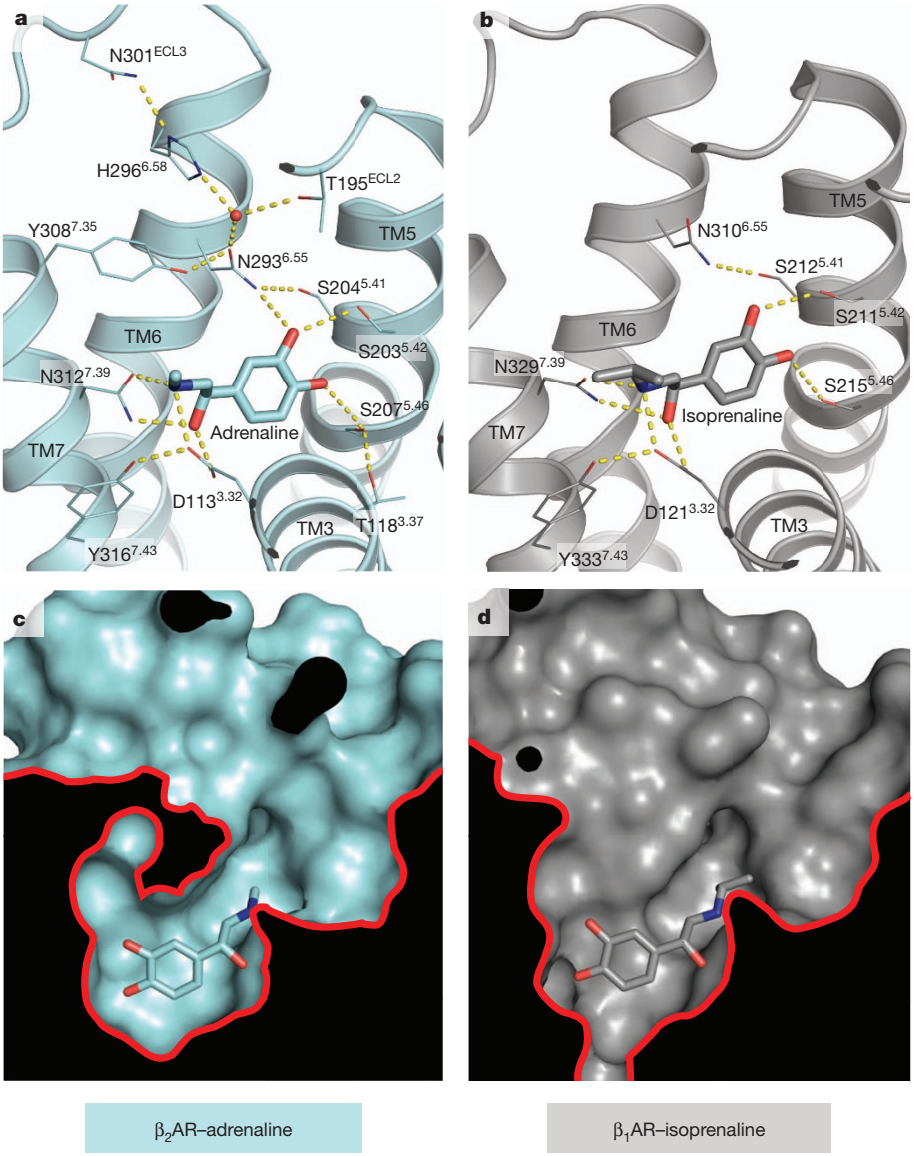

Figure 4 | Activation by catecholamine agonists. **a–d**, For the first time, structures of catecholamine-bound adrenergic receptors in active and inactive conformations can be compared. **a**, The structure of β_2AR in an active conformation bound to the agonist adrenaline reveals an extended polar contact network linking the orthosteric site to ECL2 and 3, whereas the structure of thermostabilized β_1AR in an inactive conformation bound to a similar catecholamine agonist, isoprenaline, shows a far more limited polar network. **c**, Likewise, a surface view of the active-state structure (**c**) shows a substantial contraction of the binding site compared with the inactive β_1AR structure (**d**).

bonding with Asn 293$^{6.55}$ in the receptor conformation observed in the BI167107-bound structure. To maintain the corresponding hydrogen bond between Asn 293 and the *meta* hydroxyl moiety on the catechol ring, the receptor undergoes a 1.2 Å shift in the extracellular side of TM6, which bends towards the ligand (Fig. 3c). This shift alters the hydrogen-bonding network in this region and thereby causes a change in the conformation of His 296$^{6.58}$. For adrenaline-bound β_2AR, the TM6 conformational change is further propagated towards the extracellular side of the receptor, leading to a conformational rearrangement in extracellular loop 3 (ECL3; Fig. 3d). This change also alters the extracellular surface of the receptor, with adrenaline-bound β_2AR having a contracted extracellular vestibule (Supplementary Fig. 8).

The relatively subtle differences in receptor conformation observed for the different co-crystallized agonists suggest that the activation mechanism of the β_2AR is highly similar for all agonists. Much like BI167107, the catechol head groups of adrenaline and HBI engage β_2AR residues previously characterized to be important for agonist binding and receptor activation (Supplementary Fig. 9). Consistent with prior mutagenesis studies, Ser 203$^{5.42}$ and Ser 207$^{5.46}$ make hydrogen bonds with the catecholamine phenoxy moieties[16] (Fig. 3a–c), and the conformation of these residues is nearly identical to that observed for the BI167107 head group. Ser 204$^{5.43}$, which was previously thought to contact the para-hydroxy group of the catecholamine directly[16,17], engages the catecholamine head group indirectly in an extended polar network with Tyr 308$^{7.35}$ and Asn 293$^{6.55}$. However, unlike BI167107-bound β_2AR, this polar interaction network is extended by inclusion of His 296$^{6.58}$ in the catecholamine-bound receptor, suggesting that conformational rearrangement of His 296$^{6.58}$ may stabilize the slightly smaller orthosteric binding pocket observed for catecholamine agonists. The agonist-induced rearrangements in the central portion of the transmembrane segments and intracellular surface are virtually identical in all three agonist-bound structures (Fig. 3b and Supplementary Fig. 10). Structures of β_2AR bound to BI167107 and the catecholamine agonists all show very similar activation-related changes in the residues that connect the orthosteric ligand-binding pocket to the intracellular surface, suggesting that the mechanism for allosteric coupling between the orthosteric binding site and the G-protein-coupling domain is probably a conserved feature of β_2AR activation. Therefore, different

agonists stabilize the same conformational rearrangements in the receptor through different chemical interactions.

In contrast to the marked similarity in receptor conformation for all three agonists crystallized here, far more substantial conformational differences are seen relative to a previously reported structure of the thermostabilized turkey β_1-adrenoceptor (β_1AR) bound to the catecholamine agonist isoproterenol[5]. Probably due to the thermostabilization procedure, the overall receptor conformation of isoprenaline-bound β_1AR closely resembles that of the antagonist-bound, inactive β_1AR[18], as well as that of covalent-agonist-bound, inactive β_2AR[1] (Supplementary Fig. 11). Thus, a comparison of the structural changes between inactive β_1AR and active β_2AR, each bound to catecholamines, offers new insight into how agonists bind adrenoceptors both in the low-affinity state and the high-affinity, G-protein-coupled state. Within the binding pocket, isoprenaline makes a hydrogen bond with Ser $211^{5.42}$ and the β-hydroxylamine moiety engages conserved residues $Asp^{3.32}$ and $Asn^{7.39}$ in a very similar manner to the active-state structures (Fig. 4a, b). Similar interactions can occur in both active and inactive states, probably accounting for the fact that the β-hydroxylamine moiety is an important feature of both β-adrenoceptor agonists and antagonists/inverse agonists. However, the isoprenaline catechol head group engages a limited network of polar contacts in the inactive β_1AR structure, whereas adrenaline bound to active β_2AR engages an extensive polar network linking the orthosteric site to the extracellular loops (Fig. 4a). As a consequence of structural changes stabilized by this polar network, the catechol head group of adrenaline is nearly completely enclosed within the orthosteric binding pocket of activated β_2AR (Fig. 4c). In comparison, isoprenaline bound to inactive β_1AR is highly exposed to the extracellular solvent and is slightly displaced towards the extracellular side of the receptor (Fig. 4d). Thus, in β-adrenoceptors, the combination of a more extensive polar network and a smaller binding pocket probably accounts for the enhanced agonist affinity seen in the presence of either G_s or G protein mimetic nanobodies. Moreover, such differences between active and inactive structures highlight the importance of active-state GPCR crystal structures in understanding the structural basis for agonist activity.

In conclusion, the use of new approaches in combinatorial biology has led to the development of Nb6B9, an exceptionally high-affinity GPCR-stabilizing nanobody. This molecule exhibits enhanced affinity for β_2AR relative to wild-type Nb80, and it enabled the crystallization of β_2AR in complex with three different agonists with diverse chemical structures and a wide range of affinities. The use of such high-affinity crystallization chaperones may be generally useful in the determination of active-state structures of GPCRs bound to low-affinity agonists. The crystallographic studies presented here reveal subtle, ligand-specific differences in receptor conformation superimposed on the backdrop of an overall conserved agonist-binding mode and activation mechanism, offering new insight into how chemically diverse agonists can activate a single receptor.

METHODS SUMMARY

Nb80 was displayed on the surface of EBY100 yeast as an N-terminal fusion to Aga2p, and an affinity-maturation library was generated by assembly PCR. Yeast were stained with detergent-solubilized receptor, and selections were carried out using magnetic-activated cell sorting. For crystallography, the β_2AR with an N-terminal T4 lysozyme (T4L) fusion was expressed in Sf9 insect cells and purified by ligand-affinity chromatography. Nb80 and Nb6B9 were expressed in the *Escherichia coli* periplasm and purified by Ni-NTA chromatography. For crystallization, T4L–β_2AR was incubated with ligand, followed by the addition of excess Nb6B9 and purification by gel filtration. The purified complex was reconstituted into the lipidic cubic phase and crystallized. Diffraction data were collected at Advanced Photon Source GM/CA beamlines 23ID-B and 23ID-D, and the structures were solved by molecular replacement.

Online Content Any additional Methods, Extended Data display items and Source Data are available in the online version of the paper; references unique to these sections appear only in the online paper.

Received 14 May; accepted 13 August 2013.
Published online 22 September 2013.

1. Rosenbaum, D. M. *et al.* Structure and function of an irreversible agonist–β_2 adrenoceptor complex. *Nature* **469,** 236–240 (2011).
2. Xu, F. *et al.* Structure of an agonist-bound human A_{2A} adenosine receptor. *Science* **332,** 322–327 (2011).
3. White, J. F. *et al.* Structure of the agonist-bound neurotensin receptor. *Nature* **490,** 508–513 (2012).
4. Lebon, G. *et al.* Agonist-bound adenosine A_{2A} receptor structures reveal common features of GPCR activation. *Nature* **474,** 521–525 (2011).
5. Warne, T. *et al.* The structural basis for agonist and partial agonist action on a β_1-adrenergic receptor. *Nature* **469,** 241–244 (2011).
6. Venkatakrishnan, A. J. *et al.* Molecular signatures of G-protein-coupled receptors. *Nature* **494,** 185–194 (2013).
7. Nygaard, R. *et al.* The dynamic process of β_2-adrenergic receptor activation. *Cell* **152,** 532–542 (2013).
8. Rasmussen, S. G. *et al.* Crystal structure of the β_2 adrenergic receptor–Gs protein complex. *Nature* **477,** 549–555 (2011).
9. Rasmussen, S. G. *et al.* Structure of a nanobody-stabilized active state of the β_2 adrenoceptor. *Nature* **469,** 175–180 (2011).
10. Caffrey, M. & Cherezov, V. Crystallizing membrane proteins using lipidic mesophases. *Nature Protocols* **4,** 706–731 (2009).
11. Deupi, X. *et al.* Stabilized G protein binding site in the structure of constitutively active metarhodopsin-II. *Proc. Natl Acad. Sci. USA* **109,** 119–124 (2012).
12. Schneider, E. H., Schnell, D., Strasser, A., Dove, S. & Seifert, R. Impact of the DRY motif and the missing "ionic lock" on constitutive activity and G-protein coupling of the human histamine H_4 receptor. *J. Pharmacol. Exp. Ther.* **333,** 382–392 (2010).
13. Elgeti, M. *et al.* Conserved $Tyr223^{5.58}$ plays different roles in the activation and G-protein interaction of rhodopsin. *J. Am. Chem. Soc.* **133,** 7159–7165 (2011).
14. Goncalves, J. A. *et al.* Highly conserved tyrosine stabilizes the active state of rhodopsin. *Proc. Natl Acad. Sci. USA* **107,** 19861–19866 (2010).
15. Serrano-Vega, M. J., Magnani, F., Shibata, Y. & Tate, C. G. Conformational thermostabilization of the β_1-adrenergic receptor in a detergent-resistant form. *Proc. Natl Acad. Sci. USA* **105,** 877–882 (2008).
16. Strader, C. D., Candelore, M. R., Hill, W. S., Sigal, I. S. & Dixon, R. A. Identification of two serine residues involved in agonist activation of the β-adrenergic receptor. *J. Biol. Chem.* **264,** 13572–13578 (1989).
17. Liapakis, G. *et al.* The forgotten serine. A critical role for $Ser\text{-}203^{5.42}$ in ligand binding to and activation of the β_2-adrenergic receptor. *J. Biol. Chem.* **275,** 37779–37788 (2000).
18. Warne, T. *et al.* Structure of a β_1-adrenergic G-protein-coupled receptor. *Nature* **454,** 486–491 (2008).

Supplementary Information is available in the online version of the paper.

Acknowledgements We thank D. Hilger for critical reading of the manuscript. We acknowledge support from the Stanford Medical Scientist Training Program (A.M. and A.M.R.), the American Heart Association (A.M.), the National Science Foundation (A.C.K.), the Ruth L. Kirschstein National Research Service Award (A.M.R.), National Institutes of Health grants NS02847123 and GM08311806 (B.K.K.), from the Mathers Foundation (B.K.K., W.I.W. and K.C.G.), and from the Howard Hughes Medical Institute (K.C.G.).

Author Contributions A.M.R. designed and performed yeast display staining and selection experiments, nanobody expression, purification and characterization on yeast and by SPR. A.M. and A.C.K. designed and performed receptor expression, purification, radioligand-binding experiments and crystallography experiments. M.D.E. performed crystallization experiments with adrenaline-bound β_2AR under the supervision of A.M. and A.C.K. The manuscript was written by A.M.R., A.M. and A.C.K. W.I.W. supervised structure refinement. K.C.G. and B.K.K. supervised experiments, and B.K.K. supervised manuscript preparation.

Author Information Coordinates and structure factors for the β_2AR–Nb6B9 complexes with BI167107, HBI and adrenaline ligands are deposited in the Protein Data Bank under accession codes 4LDE, 4LDL and 4LDO, respectively. Reprints and permissions information is available at www.nature.com/reprints. The authors declare competing financial interests: details accompany the full-text HTML version of the paper at www.nature.com/nature. Readers are welcome to comment on the online version of the paper. Correspondence and requests for materials should be addressed to K.C.G. (kcgarcia@stanford.edu) or B.K.K. (kobilka@stanford.edu).

METHODS

β_2AR expression and purification. Human β_2AR bearing an N-terminal Flag epitope tag and truncated after residue 365 was expressed in Sf9 insect cells using the BestBac baculovirus system (Expression Systems). Cells were infected at a density of 4×10^6 cells ml^{-1}, then incubated for two days at 27 °C. Receptor was extracted as described previously[19]. Receptor was first purified by Flag affinity chromatography, then labelled with a tenfold molar excess of biotin-PEG_{11}-maleimide (Thermo Scientific), which reacts with the endogenous residue Cys 265. After a 1 h incubation at room temperature (22 °C), unlabelled receptor was blocked with 2 mM iodoacetamide for 15 min and then purified by alprenolol sepharose chromatography to isolate only functional receptor. Alprenolol sepharose eluate was concentrated on Flag affinity resin, and then washed with ligand-free buffer for 30 min at room temperature to eliminate bound alprenolol. Detergent was gradually exchanged from dodecyl maltoside (DDM) to lauryl maltose neopentyl glycol (MNG) by washing in buffer containing decreasing amounts of DDM and MNG at a fixed concentration of 0.1% (w/w). Receptor was eluted, aliquoted, and frozen in 20% glycerol.

Display and functional evaluation of Nb80 on yeast. Nb80 was cloned into the C-terminal Aga2 yeast-display vector pYAL[20] and transformed and displayed on yeast as previously described[21]. Induced yeast displaying Nb80 were washed with PBE buffer (phosphate buffered saline with 0.5 mM EDTA and 0.5% BSA) supplemented with 0.02% MNG detergent (PBEM buffer) and stained with varying concentrations of biotinylated receptor bound to either BI167107 or carazolol for 1 h at 4 °C. The yeast were then washed with PBEM buffer and stained with Alexa-647-conjugated streptavidin for 15 min at 4 °C. Mean cell fluorescence was measured using the FL-4 channel of an Accuri C6 flow cytometer.

Affinity maturation of Nb80. The affinity maturation library was prepared by assembly PCR with oligonucleotide primers (Supplementary Table 3) containing degenerate codons at 15 distinct positions (Supplementary Fig. 2). The PCR product was further amplified with primers containing 50 base pairs of homology to pYal. Mutagenic nanobody DNA and linearized pYAL vector were co-electroporated into EBY100 yeast to yield a library of 0.8×10^8 transformants.

For the first round of selection, 1.0×10^9 yeast induced with SGCAA medium were washed with PBEM buffer and then resuspended in 5 ml of PBEM buffer containing 200 nM biotinylated β_2AR bound to BI167107. After 1 h of incubation at 4 °C with rotation, yeast were washed with PBEM buffer, and then stained with Alexa-647-conjugated streptavidin in PBEM buffer for 15 min at 4 °C. Yeast were washed again with PBEM buffer and magnetically labelled with 250 µl anti-Alexa-647 microbeads (Miltenyi) in 4.75 ml PBEM buffer for 15 min at 4 °C. Yeast were washed a final time and labelled yeast were isolated by magnetic selection with an LS column (Miltenyi) pre-equilibrated with PBEM buffer. Magnetically sorted yeast were resuspended in SDCAA medium and cultured at 30 °C.

Rounds 2–6 were selected in a similar manner, with the following modifications. Before positive selection with agonist-occupied β_2AR, negative selection with antagonist-bound receptor was performed to select for clones that maintained a preference for the active state of the β_2AR. Briefly, 1.0×10^8 yeast were washed with PBEM buffer and resuspended in 500 µl PBEM buffer containing 1 µM biotinylated β_2AR bound to carazolol. Yeast were incubated at 4 °C for 1 h, then labelled with Alexa-647- or PE-conjugated streptavidin, and magnetically labelled with 50 µl of the respective anti-fluorophore microbeads (Miltenyi) in 450 µl PBEM buffer. Magnetically labelled yeast were applied to an LS column and the depleted flow-through was collected for subsequent positive selection. In this manner, yeast clones binding the 'inactive', antagonist-occupied receptor were discarded. Positive selections on 'active', agonist-occupied receptor were performed as for round 1, but in a staining volume of 500 µl and with successively decreasing concentrations of BI167107-bound β_2AR: 200 nM receptor for rounds 2 and 3, 20 nM receptor for round 4, and 1 nM receptor for round 5. For round 6, positive selection was performed by a kinetic selection strategy to select for clones with the slowest off-rates (Supplementary Fig. 3). Briefly, yeast were stained with 200 nM biotinylated BI167107-bound β_2AR for 1 h, washed with PBEM, and then resuspended in 500 µl PBEM containing 15 µM Nb80. The cells were incubated at 25 °C for 155 min, after which they were washed with ice-cold PBEM and stained with fluorescent streptavidin. Enrichment with magnetic separation for rounds 2–6 was performed as for round 1, but with 50 µl anti-fluorophore magnetic microbeads with 450 µl PBEM buffer. After round 6, post-sorted yeast were plated onto SDCAA-agar plates, colonies were picked and cultured in liquid SDCAA medium, and the plasmids encoding the nanobodies were isolated with a ZymoPrep Yeast Plasmid Miniprep II kit (Zymo Research) and sequenced.

Expression and characterization of Nb80 and Nb6B9. Nanobodies were cloned into the periplasmic expression vector pET26b, containing an N-terminal signal sequence and a C-terminal 8× histidine tag, and transformed into BL21(DE3) Rosetta2 *Escherichia coli* (Novagen). Cells were induced in Terrific Broth at an $OD_{600\,nm}$ of 0.8 with 1 mM IPTG and incubated with shaking at 22 °C for 24 h. Periplasmic protein was obtained by osmotic shock and the nanobodies were purified using nickel-nitrilotriacetic acid (Ni-NTA) chromatography[9]. For crystallography, Nb6B9 was digested overnight with 1:50 (w/w) carboxypeptidase A (Sigma) to remove the His tag, then purified by size-exclusion chromatography over a Sephadex S200 size-exclusion column.

SPR experiments were conducted with a Biacore T100 at 25 °C. Protein concentrations were determined by 280 nm absorbance with a Nanodrop2000 spectrometer (Thermo Scientific). Biotinylated BI167107-bound β_2AR was immobilized on an SA sensorchip (GE) at a relative unit maximum (R_{max}) of nanobody bindingof approximately 40 RU. Biotinylated tiotropium-bound M_2 muscarinic receptor was immobilized with an RU value matching that of the reference surface to control for nonspecific binding. Measurements were made using serial dilutions of Nb80 or Nb6B9 in HBSM (10 mM HEPES pH 7.4, 150 mM NaCl, 0.01% MNG) using single-cycle kinetics. All data were analysed with the Biacore T100 evaluation software version 2.0 with a 1:1 Langmuir binding model.

Radioligand-binding assays were performed using purified β_2AR reconstituted into high-density lipoprotein particles comprised of apolipoprotein A1 and a 3:2 (mol:mol) mixture of POPC:POPG lipid[22]. Binding experiments with G protein were performed as previously described[8]. Binding reactions were 500 µl in volume, and contained 50 fmol functional receptor, 0.5 nM ^{3}H dihydroalprenolol (^{3}H-DHA), 100 mM NaCl, 20 mM HEPES pH 7.5, 0.1% bovine serum albumin, and ligands and nanobodies as indicated. Reactions were mixed, then incubated for 4 h at room temperature before filtration with a Brandel 48-well harvester onto a filter pre-treated with 0.1% polyethylenimine. Radioactivity was measured by liquid scintillation counting. All measurements were performed in triplicate, and are presented as means ± standard error of the mean.

Purification and crystallization of β_2AR–Nb6B9 complexes. Human β_2AR fused to an N-terminal T4 lysozyme[23] was expressed in Sf9 insect cells and purified as described earlier. After purification by alprenolol sepharose, the receptor was washed extensively with 30 µM of the low-affinity antagonist atenolol while bound to Flag affinity resin to fully displace alprenolol, then washed and eluted in buffer devoid of ligand to produce a homogeneously unliganded preparation. The receptor was then incubated for 30 min at room temperature with a stoichiometric excess of ligand (HBI or BI167107). A 1.3-fold molar excess of Nb6B9 was then added, and the sample was dialysed overnight into a buffer consisting of 100 mM sodium chloride, 20 mM HEPES pH 7.5, 0.01% lauryl maltose neopentyl glycol detergent, and 0.001% cholesteryl hemisuccinate. In each case, ligand was included in the dialysis buffer at 100 nM concentration or higher. The sample was then concentrated using a 50 kDa spin concentrator and purified over a Sephadex S200 size-exclusion column in the same buffer as for dialysis, and the β_2AR–Nb6B9–ligand ternary complex was isolated. In the case of adrenaline, the low affinity and chemical instability of the ligand precluded overnight dialysis, so 100 µM adrenaline was added to receptor for 30 min at room temperature, then a 1.3-fold molar excess of Nb6B9 was added and the sample was incubated for 30 min at room temperature. After incubation, the sample was concentrated and immediately purified by size exclusion as described earlier.

After purification, samples were concentrated to $A_{280\,nm} = 55$ using a 50 kDa concentrator to minimize the detergent concentration in the final sample, then aliquoted into thin-walled PCR tubes at 8 µl per aliquot. Aliquots were flash frozen in liquid nitrogen and stored at −80 °C for crystallization trials. For crystallization, samples were thawed and reconstituted into lipidic cubic phase with a 1:1 mass:-mass ratio of lipid. The lipid stock consisted of a 10:1 mix by mass of 7.7 monoacylglycerol (provided by M. Caffrey) with cholesterol (Sigma). Samples were reconstituted by the two-syringe mixing method[10] and then dispensed into glass sandwich plates using a GryphonLCP robot (Art Robbins Instruments). In the case of the β_2AR–adrenaline complex, 1 mM fresh adrenaline was mixed with receptor before reconstitution. Crystals were grown using 30 nl protein/lipid drops with 600 nl overlay solution, which consisted of 18–24% PEG400, 100 mM MES pH 6.2 to pH 6.7, and 40–100 mM ammonium phosphate dibasic. Crystals grew in 1–3 days, and were harvested and frozen in liquid nitrogen for data collection.

Crystallographic data collection and refinement. X-ray diffraction data were collected at Advanced Photon Source GM/CA beamlines 23ID-B and 23ID-D. The best diffracting crystals were identified by rastering, and wedges of 1–10° were collected using a 10 µm beam with typically 2 s exposure, 0.6° oscillation, and no beam attenuation. Data collection statistics are summarized in Supplementary Table 1. Diffraction data were processed in HKL2000[24], and the structure was solved using molecular replacement with the structures of active β_2AR, Nb80 (PDB accession 3P0G), and T4 lysozyme (PDB accession 2RH1) used as search models in Phaser[25]. The resulting structure was iteratively refined in Phenix[26] and manually rebuilt in Coot[27]. Final refinement statistics are summarized in Supplementary Table 1. Figures were prepared in PyMol.

19. Kobilka, B. K. Amino and carboxyl terminal modifications to facilitate the production and purification of a G protein-coupled receptor. *Anal. Biochem.* **231,** 269–271 (1995).
20. Wang, Z., Mathias, A., Stavrou, S. & Neville, D. M. Jr. A new yeast display vector permitting free scFv amino termini can augment ligand binding affinities. *Protein Eng. Des. Sel.* **18,** 337–343 (2005).
21. Chao, G. *et al.* Isolating and engineering human antibodies using yeast surface display. *Nature Protocols* **1,** 755–768 (2006).
22. Whorton, M. R. *et al.* A monomeric G protein-coupled receptor isolated in a high-density lipoprotein particle efficiently activates its G protein. *Proc. Natl Acad. Sci. USA* **104,** 7682–7687 (2007).
23. Zou, Y., Weis, W. I. & Kobilka, B. K. N-terminal T4 lysozyme fusion facilitates crystallization of a G protein coupled receptor. *PLoS ONE* **7,** e46039 (2012).
24. Otwinowski, Z. & Minor, W. in *Methods in Enzymology* Vol. 276 (ed. Carter, C. W. Jr) 307–326 (Academic, 1997).
25. McCoy, A. J. *et al.* Phaser crystallographic software. *J. Appl. Cryst.* **40,** 658–674 (2007).
26. Afonine, P. V. *et al.* Towards automated crystallographic structure refinement with phenix.refine. *Acta Crystallogr. D* **68,** 352–367 (2012).
27. Emsley, P. & Cowtan, K. Coot: model-building tools for molecular graphics. *Acta Crystallogr. D* **60,** 2126–2132 (2004).